Nuclear Engineering and Technology 52 (2020) 1043–1050

Contents lists available at ScienceDirect

Nuclear Engineering and Technology

journal homepage: www.elsevier.com/locate/net

Original Article

Performance assessment of HEPA filter against radioactive aerosols from metal cutting during nuclear decommissioning

Min-Ho Lee, Wonseok Yang, Nakkyu Chae, Sungyeol Choi*

Department of Nuclear and Quantum Engineering, Korea Advanced Institute of Science and Technology, 291 Daehak-Ro, Yuseong-Gu, Daejeon, 34141, Republic of Korea

ARTICLE INFO

Article history:
Received 23 July 2019
Received in revised form
24 September 2019
Accepted 22 October 2019
Available online 22 October 2019

Keywords:
Radioactive aerosols
HEPA filter
Aerodynamic diameter
Metal cutting
Nuclear power plant decommissioning

ABSTRACT

Radioactive aerosols are produced during the cutting of contaminated and activated metals. They must be collected and removed by a high-performing filtration system before releasing to the environment from the decommissioning workplace. The filtration system requires regular replacement to ensure the sufficient removal of radioactive aerosols because its filtration efficiency gradually decreases. This study evaluates the efficiency and lifetime of filters while cutting metals by using a plasma arc cutter. Particularly, this study considers the aerodynamic diameter distribution of number and mass concentrations for aerosols from 6 nm to 10 μm when evaluating the performance of filters. After 20 time reuses for cutting operation performed in a cutting chamber, the removal efficiency is reduced from over 99 to below 93% at 2 μm. The results are used to analyze the lifetime of filters, the frequencies of their replacements, and impact on internal radiation dose.

1. Introduction

Many nuclear power plants (NPPs) constructed in the 1970s will be decommissioned. During the decommissioning and decontamination (D&D) of nuclear reactors and nuclear fuel cycle facilities, various types of radioactive waste can be generated [1–3]. For treating these radioactive wastes, numerous cutting operations are required for dismantling various activated metallic components. The cutting of the metallic components produces aerosols in particle size of a few nm to 10 μm, and radioactive isotopes can be trapped into the aerosols, so-called radioactive aerosols [4–8]. Once radioactive aerosols are generated, they will be dispersed in the workplace and have the potential to contribute to the internal dose of people and the radiological contamination of the environment [9]. Thus, the workplace for cutting has to be designed and operated to efficiently manage radioactive aerosols not to release to the environment by using a filtration system.

The nuclear facilities, including the D&D workplace, usually use high-efficiency particulate air (HEPA) filters to prevent the leakage of radioactive aerosols to the environment for protecting people and minimizing contamination. Most of the aerosols do not pass through the filter [10–12]. However, the aerosol particles around 300 nm in size cannot be completely removed by the filter because the HEPA filters have the lowest filtration efficiency in a region of 300 nm size [13,14]. As the removal efficiency of filters gradually decreases during operation, the filters no longer meet the requirements of HEPA filter, and they are needed to be replaced. To protect the workers, the public, and the environment at reasonable costs and acceptable waste generated, it is important to evaluate the removal efficiency of aerosols and determine the frequencies of replacements [15].

Several studies have been conducted for evaluating factors affecting filter efficiency [16–19]. However, most studies have been conducted using conventional aerosol generators, and aerosols that occur during metal cutting have not been addressed significantly. In addition, many studies have not fully considered the distribution of particle sizes for the efficiency of filters [20–22], although it is significant to understand the fraction of aerosols smaller than 0.1 μm for reducing internal radiation dose. The aerosols smaller than 0.1 μm are respirable. Dispersion and deposition behaviors are also a function of aerodynamic diameter. Moreover, there is a very limited study to evaluate the lifetime and replacement frequency of filters according to the distribution of particle sizes.

The purpose of this experimental study is to evaluate the efficiency and lifetime of HEPA filters while cutting metallic

* Corresponding author.
E-mail address: sungyeolchoi@kaist.ac.kr (S. Choi).

https://doi.org/10.1016/j.net.2019.10.017

components. A unique experimental system is used for cutting metal sheets using a plasma arc cutter, measuring the aerodynamic diameter distribution of number and mass for aerosols from metal cutting, and collecting the aerosols in HEPA filters before release. In particular, this study analyzes the reduction of filtration efficiency across a range of different particle sizes from 6 nm to 10 μm. Also, the pressure drop across the filter is measured and used to suggest a method to determine the lifetime of the filter or the frequencies of its replacements.

2. Material and methods

2.1. Aerosol chamber and sampling pipe for collecting aerosol

We designed the isolated aerosol chamber for collecting generated aerosol particles without leakage outside. The aerosol chamber was designed with a size of 1.3 m wide, 1 m long, and 0.66 m high. Fresh air flows continuously into the chamber through the air inlet tube with a HEPA filter installed on the side of the chamber. The aerosols generated by metal cutting is released through a sampling pipe in which the opposite side of the inlet tube. The end of the sampling pipe is connected to a blower pump system (Fig. 1).

The sampling line was designed for minimizing particle losses which would be a measurement error [23]. To minimize particle losses in the sampling line caused by gravitational settling, shock, and thermoplastic forces, the sampling line was installed as short as possible without bending [24]. Also, the inner surface of the chamber and sampling tube was coated to prevent particle losses by sticking to the surface.

2.2. Automatic metal cutting system

A plasma cutter (Powermax 125, Hypertherm) was selected to cut a metal plate. The plasma cutter was fixed in the center of the chamber ceiling. The plasma cutting device operated up to 125A current power by supplying compressed air. A movable table controlled by the servo-motor system on X-axis may adjust the speed of the metal cutting. A PLC panel connecting the plasma arc cutter to the movable table provides the program to set the placement and moving speed of the workpiece. This allows the movement of the workpiece to be reproduced and controlled precisely (Fig. 2).

Fig. 1. The aerosol measurement system for metal cutting in KAIST Nuclear Fuel Cycle Lab.

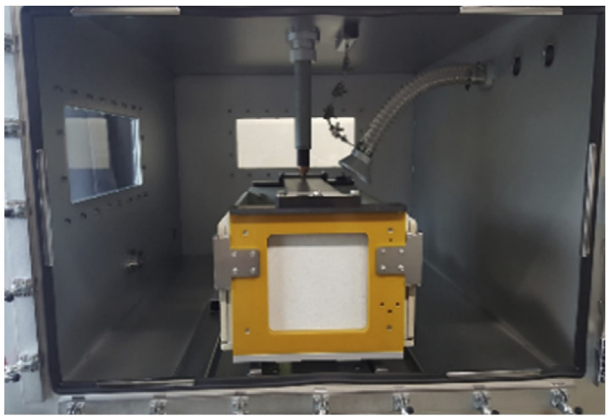

Fig. 2. Plasma cutting device (Powermax 125, Hypertherm) and moving table controlled by the servo-motor system.

2.3. Detection and measurement of metal-containing aerosols

The measurement of the aerosol is performed using an electrical low-pressure impactor (ELPI+, DEKATI) and a diluter (eDiluter, DEKATI). All aerosol particles which have the size from 6 nm up to 10 μm were collected at each of 15 different size stages. Unlike a typical cascade impactor, a unipolar corona charger in ELPI+ allows aerosol particles to have an electrical charge. For this reason, ELPI+ has the advantage of real-time monitoring, while the concentration of measurable aerosols has a maximum limit for each step. Since the concentration of aerosols generated by metal cutting is higher than the measurement limit at some of impactor stage regions (Fig. 3), the diluter was used for reducing concentration. The dilution factor of the diluter was identified as 64 at 1013 mbar.

The measured distribution data was converted into the normalized form to compare each distribution form directly. Normalized number per logarithmic diameter denoted by a "(dN/N)/dlogD_p" and normalized mass per logarithmic diameter denoted

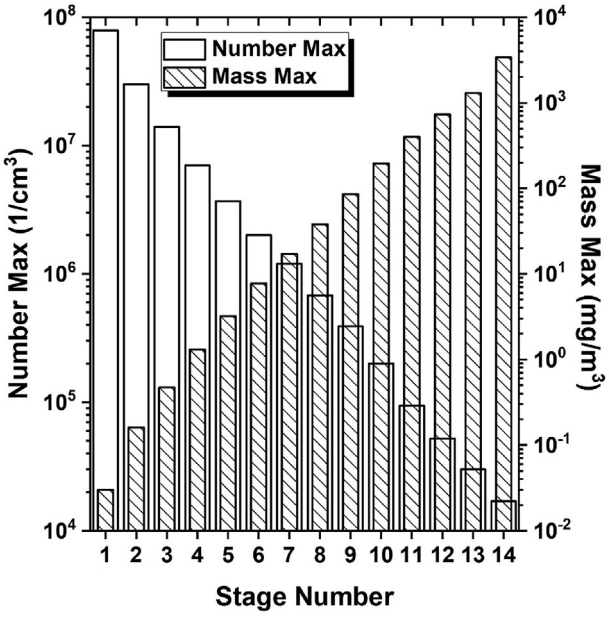

Fig. 3. Maximum count and mass concentration limits for each stage of the ELPI+ specifications. The number and mass of aerosol that exceed the limits of each stage are incorrectly recognized as maximum values.

by a "(dM/M)/dlogD$_p$" were plotted along the Y-axis.

$$\frac{dN}{N \times d\,\log D_p} = \frac{dN}{N \times \left(\log D_{p,u} - \log D_{p,l}\right)} \quad (1)$$

where N is the total number of particles in all stages of the impactor, dN is the number of collected particle in each stage of the impactor.

$$\frac{dM}{M \times d\,\log D_p} = \frac{dM}{M \times \left(\log D_{p,u} - \log D_{p,l}\right)} \quad (2)$$

where M is the total mass of particles in all stages of the impactor, dM is the mass of particles collected particle in each stage of the impactor, and dlogD$_p$ is the difference in the log of the aerodynamic diameter width. dlogD$_p$ is calculated by subtracting the log of the lower stage aerodynamic diameter (logD$_{p,l}$) from the log of the upper stage (logD$_{p,u}$) in ELPI+ properties (Table 1).

The aerodynamic diameter (Dp) corresponding to the x-axis is on a log scale because of the broad range of the measurement from 6 nm up to 10 μm size. Also, dlogD$_p$ could be changed dependent on measurement resolution. For this reason, the size distribution function is usually plotted as dN/dlogDp to avoid measurement error resulted from the difference in measurement resolution of the equipment. The normalized distribution form ((dN/N)/dlogDp) is needed to avoid confusing data interpretation resulted from both the different total counted value as well as the different resolution of a measurement system [25].

2.4. Aerosol filtration system with HEPA filter

We assumed that an operator would cut the stainless steel in lengths of 3 cm with a plasma arc torch at given chamber size, and this process was defined as "unit cut" in our cutting scenario. The cutting process repeats the same operation up to 20 times using the same HEPA filter without exchanging. The number and mass of aerosols generated during each cutting were measured by ELPI+.

The HEPA filter (Woosung HI-VAC, Korea) is a custom-made filter by folding the fabric to form a cylindrical shape. For coupling with the sample pipe, the HEPA filter was mounted in a metal basket which has the same diameter as the pipe. The HEPA filter was installed in front of the sampling port to measure particles downstream of the filter (Fig. 4). When measuring downstream aerosols of the HEPA filter, the majority of aerosols are captured inside the filter, so we connected ELPI+ to sampling pipe directly without using the diluter.

Table 1
Nominal impactors specification of ELPI+.

Stage Number	D50% (μm)	Di (μm)	dlogDp
1	0.006	0.00936	0.386202
2	0.0146	0.020541	0.296545
3	0.0289	0.039541	0.272299
4	0.0541	0.071539	0.242694
5	0.0946	0.121091	0.214441
6	0.155	0.199198	0.217908
7	0.256	0.312308	0.172685
8	0.381	0.478918	0.198672
9	0.602	0.755046	0.196753
10	0.947	1.242421	0.235838
11	1.63	2.006514	0.180509
12	2.47	3.002582	0.169596
13	3.65	4.423121	0.166872
14	5.36	7.277142	0.265592
15	9.88	–	–

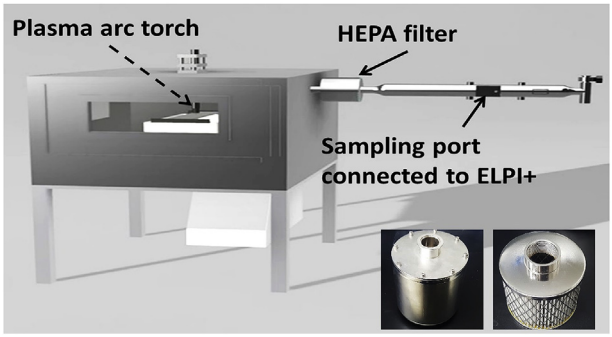

Fig. 4. The aerosol measurement system for measuring particles downstream of the filter. The handmade HEPA filter and filter basket were installed in front of the sampling port. Using flexible plastic tube, generated aerosols were transported to the inlet of ELPI+.

3. Results

3.1. Aerodynamic diameter distribution of mass and number according to the existence of filter

In order to compare the particle size distributions between the concentration of aerosols with and without filters, particle size distribution is reported as a normalized concentration. Fig. 5 shows the particle size distributions between the concentration of pre-filter and post-filter. Without the filtration system, the normalized number distribution has a single peak around 0.1 μm regions, whereas the mass distribution shows a bimodal distribution with peaks around 0.3 μm and 9 μm (Fig. 5 (a)). In the case of the post-filter streamline, the number distribution is quite similar in having a single peak. However, there is a significant difference between the mass distribution of aerosols without filtration system and that of filtered aerosols. Unlike the previous one, the filtered aerosols show a trimodal distribution with peaks around 0.3 μm, 3 μm, and 9 μm (Fig. 5 (b)).

3.2. Life-time of HEPA filter on metal cutting condition

Fig. 6 shows the number and mass aerodynamic distribution of aerosol when the same HEPA filter was used up to 20 times cycle without replacements. Despite the repeated process, it showed quite similar the number distribution with a single peak at 0.1 μm regions. As the cutting process was repeated, the peak tended to shift to 0.3 μm. In mass distribution, the peak value tended to increase from 0.3 μm as the number of filter reusable increased.

The relationships between the total counted number of aerosols and the number of filter reuses are fitted by the linear equations. As the number of reusing the same HEPA filter without exchanging increases, both the number and the mass of particles in filter downstream increase in exact proportion (Fig. 7). As the number of filter reuses increased to 20, the number concentration of aerosols passed through the filter increased by about 3 times and the mass concentration was about 10 times higher than that of the new filter.

3.3. Aerosol removal efficiency of HEPA filter

The beta ratio is one of the indices that can be used to show a removal efficiency of filter easily. The beta ratio is defined as the ratio of influent particle number to effluent particle number [26]. It follows that the higher the value of the beta ratio, the more particles of the specified size or greater are retained on the filter.

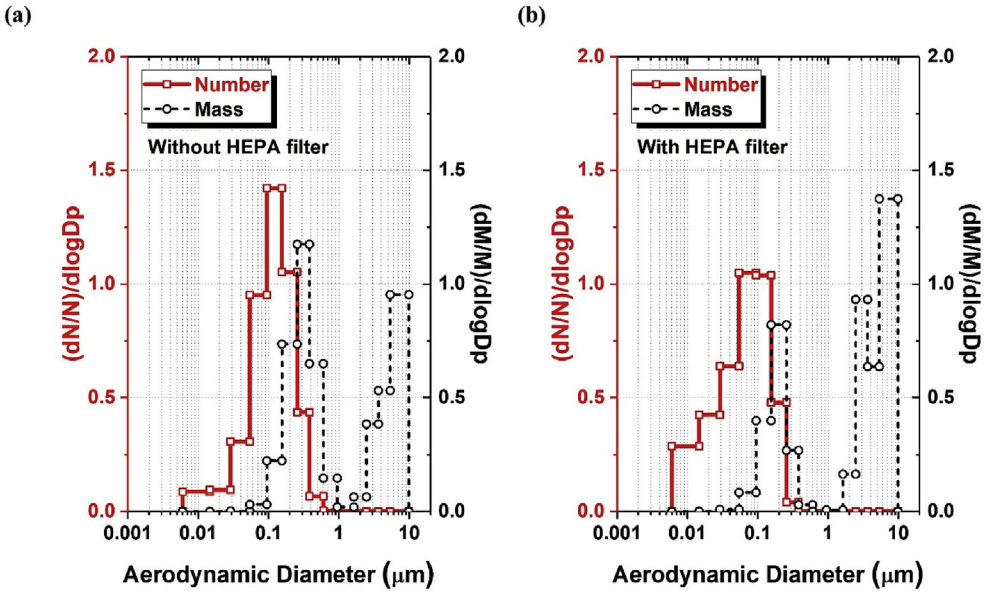

Fig. 5. Counted number and mass aerodynamic diameter distribution of stainless-steel cut with the plasma cutter. (a): The particle size distributions of pre-filter stream line (without filter), (b): The particle size distributions of post-filter stream line (with filter).

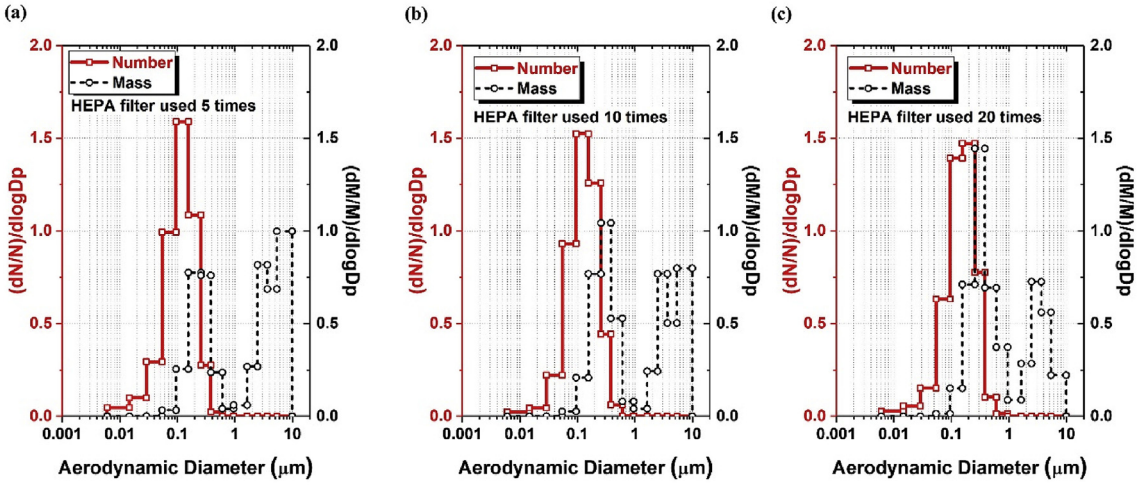

Fig. 6. Counted number and mass aerodynamic diameter distribution of stainless-steel cut with the plasma cutter without exchanging HEPA filter. (a): Test filter reused 5 times, (b): 10 times, (c):.20 times.

$$\beta_x = \left(\frac{C_{u,x}}{C_{d,x}}\right) \tag{3}$$

Where β_x is the beta ratio for particles larger than x μm, $C_{u,x}$ is the concentration of upstream particles larger than x μm, and $C_{d,x}$ is the concentration of downstream particles larger than x μm.

The ratio of upstream to downstream concentrations at a given particle size is then used to determine the particle size removal efficiency (PSE) at that particle size [27]. For example, if the upstream concentration and the downstream concentration particles of test filter are C_u and C_d, the particle size removal efficiency is determined as:

$$\mathrm{PSE} = \left(1 - \frac{C_d}{C_u}\right) \times 100\,\% \tag{4}$$

In the size area corresponding to ultrafine dust (PM 2.5), the removal efficiency was highest at 99.85% when the new filter was used. Subsequently, it consistently decreased as the number of reuse filters increased and decreased by 99.07% for filters used 20 times (Fig. 8) (Table 2). The removal efficiency of aerosols below 10 μm, which can be measured with ELPI, was similar to that of those below 2.5 μm above. As a result, our custom-made filter had up to 99.86% efficiency and tended to gradually decrease as the number of reuses increased (Table 3).

The overall filter efficiency is over 99%, but the particle removal efficiency could be greatly reduced at certain particle size. As shown in Fig. 9, the efficiency of the new filter at 0.02 μm had a minimum value of 99.73%, and the efficiency of the reused filters dramatically decreased locally at 0.3 and 2 μm values. In particular, the efficiency of the filters reused 20 times had decreased substantially, even reaching 93.3% level at 2 μm size regions.

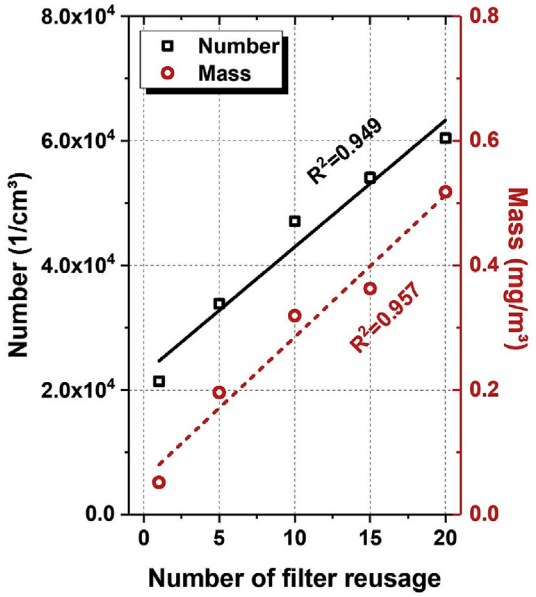

Fig. 7. The number and the mass of particles in filter downstream depending on number of filter reused. The linear fitting lines with the R-squared values are calculated by using OriginPro program.

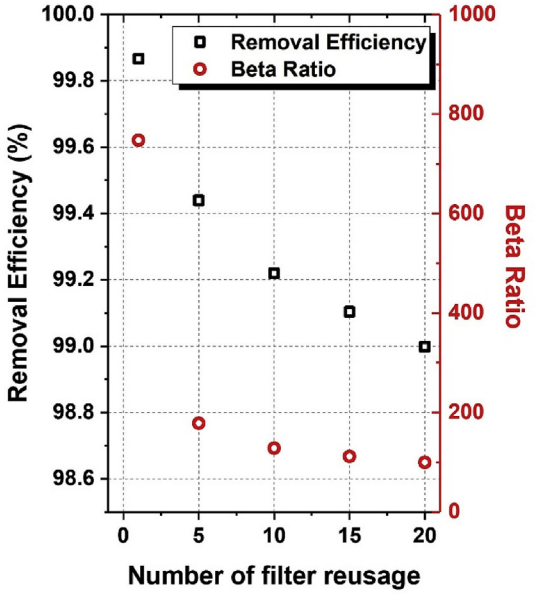

Fig. 8. Particle removal efficiency and beta ratio versus filter reuse number. As the number of filter reused up to 20 times, the particle removal efficiency tends to decrease continuously.

4. Discussion

HEPA filters are commonly used in many industries to prevent harmful aerosols from entering the surrounding ecosystem and the operator's respiratory tract. HEPA filters are usually rated according to one of the two most common classification systems; the EN-1822 standard issued by Eurovent 1 and the minimum efficiency reporting value (MERV) standard issued by the American Society of Heating [11].

4.1. HEPA filter performance depending on aerodynamic diameter

A filter test has been traditionally performed by measuring the particle penetration ratio of a thermally generated dioctyl-phthalate (DOP) aerosol [28]. The HEPA filter should be required to remove at least 99.95% or 99.97% of particles that are 0.3 μm in diameter at rated flow. In theory, the most penetrating particle size (MPPS) in the fibrous filter was identified to be between 0.1 μm and 0.3 μm [14]. That is the reason why the 0.3 μm size selected a critical point for the definition of HEPA filter. Fiber filters essentially remove an aerosol particle using one of the following five basic mechanisms: (1) direct interception, (2) inertial impaction, (3) diffusion, (4) electrostatic attraction, and (5) gravitational settling.

Inertial impaction occurs when the particle cannot follow a flow line because of sufficient momentum with going straight toward the filter elements. Direct interception can occur if the particle follows a flow line which is close enough to contact the filter elements [29]. For this reason, relatively larger particles having the chance to escape from the gas stream are likely to follow the inertial impaction mechanism. By contrast, the smaller particles may be likely to be captured by impaction at the closest point. If most particles are less than 1 μm, diffusion (Brownian motion) and electrostatic attraction are dominant because of higher molecular mobility other than the two mechanisms, as mentioned above [30]. A gravitational settling may also contribute to particle capture. However, gravitational settling is not relevant in the nano-sized aerosol region. Brownian diffusion is a random motion of small particles. It occurs predominantly in particle smaller than about 0.1 μm [12]. Electrostatic precipitation is based on the electrostatic attraction between a single charged particle and an opposite polarity of collection device [31]. The aerosol capture mechanisms of the filter are quite complicated, as described in the above paragraphs. But in a nutshell, particles larger than 1 μm can be mainly filtered by impaction and direct interception, whereas particles from 0.001 to 1 μm are removed by diffusion and electrostatic separation [32]. However, this relationship of the capture mechanisms and the particle size can only be explained theoretically, and the particle removal efficiency of the actual filter can vary depending on the physical composition of the filter, the particle flow rate, and the properties of aerosols.

As shown in Fig. 9, the filter efficiency for 0.3 μm sized particles

Table 2
Comparison of filter particle removal performance for PM 2.5 (under 2.5 μm diameter).

Filter Reuse Number	Influent Particle Count (#/cm³)	Effluent Particle Count (#/cm³)	Removal Efficiency (%)	Beta Ratio
0 (New filter)	5,494,213	8,009.799	99.85421	685.9364
5		32,042.88	99.41679	171.4644
10		42,874.41	99.21964	128.1467
15		48,076.34	99.12496	114.2810
20		50,897.13	99.07362	107.9474

Table 3
Comparison of filter particle removal performance for PM 10 (under 10 μm diameter).

Filter Reuse Number	Influent Particle Count (#/cm^3)	Effluent Particle Count (#/cm^3)	Removal Efficiency (%)	Beta Ratio
0 (New filter)	6,034,207	8,077.190	99.86614	747.0677
5		33,832.61	99.43932	178.3548
10		47,095.05	99.21953	128.1283
15		54,069.63	99.10395	111.6007
20		60,434.75	98.99846	99.8467

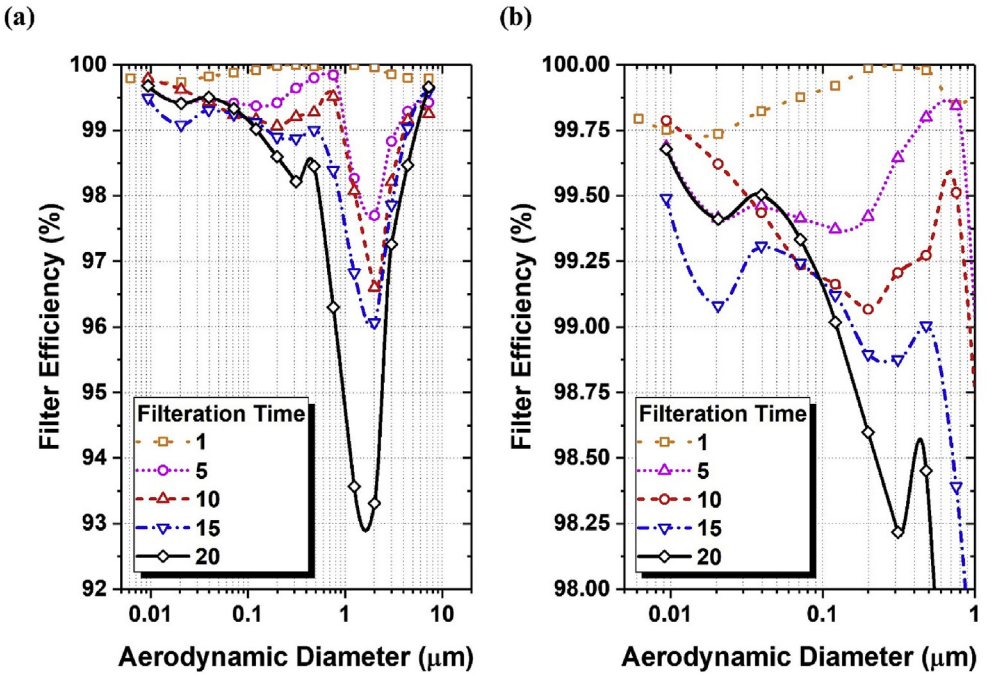

Fig. 9. Particle removal efficiency versus particle size for HEPA filter. (a): 0.06 nm to 10 μm size distribution, (b) Magnify graph: To view distribution trends of 0.06 nm–1 μm.

is 99.99%, which appears to meet the HEPA filter requirements. Unlike filter theory, however, MPPS was identified in the 0.02 μm sized area, and the filter efficiency was 99.73%. Also, the new filter particle removal performance of PM 10 and PM 2.5 were 99.86% and 99.85% respectively (Tables 2 and 3), which is not strictly satisfied with the minimum efficiency of HEPA filters (99.95% or 99.97%). It is assumed that the types of aerosols used in the filter test were different, and the flow rate was also very different from the typical filter test. The test has been used relatively sophisticated equipment to manufacture DOP aerosols of homogenous size (0.3 μm) to form an almost single dispersion aerosol. However, we collected metal-containing aerosols from the actual metal cutting process. Unlike DOP aerosols, metal-containing aerosols have not homogenous size distribution and also have high density resulting in a binomial mass distribution with peaks around 0.3 μm and 9 μm (Fig. 5(a)). It is well established that increasing aerosol velocity results in a shift in filter MPPS to smaller particle sizes, both from theoretical and experimental perspectives [33,34]. The inertial impaction would become increasingly important at sufficiently high velocities. Thus, the MPPS would shift from 0.3 μm to 0.02 μm in a smaller size. For example, the filter test controlled the fluid flow at a speed of a few cm/s to avoid product damage of the filter. But, in this experiment, relatively large flow rates were used to account for the actual working environment at a rate of a few m/s.

4.2. Particle removal efficiency of HEPA filter according to filter usage time

As aerosol particles accumulate in the filter, the permeability of HEPA filter decreases and the force acting on the aging substance increases consequently [12]. Therefore, the pressure drop in the filter increases due to the dust load and the weakening of the filter material. Except for electrostatic effects, the efficiency of the filter may increase temporarily as the dust load increases. However, the efficiency of the filter decreases because the flow rate decreases when the pressure drop across filter reaches a certain point. In high-pressure environments, filter bypasses can occur when air passes around the filter or through other unintended paths, and the filter rupture may be carried out in severe cases. Hence, filter replacement is determined by measuring or predicting the pressure drop [22]. Until now, the decision to replace the filter by pressure drop does not reflect the physical and chemical properties of aerosols that actually come through the filter.

To overcome these limitations, the efficiency of the filter was calculated by measuring aerosols from downstream of the test filter according to filter usage time in this study. It is experimentally confirmed that MPPS of filters can be formed in different areas from theoretical values, and filter efficiency continues to decrease as filter usage time increases. When the test filter was reused for 20 times, the number concentration of aerosol was 3 times higher than using the new test filter. In addition, the total filter efficiency

dropped from 99.86% to 98.99% (Table 3). In areas less than 1 μm size, MPPS is 0.2–0.3 μm when reusing filters and is the same as theoretical values. As the number of reuses increases, the filter efficiency decreases at 0.2–0.3 μm. Finally, the 20 times reused filter efficiency at 0.3 μm is reduced to 98.2% which is about 1.7% lower than that of the new filter (Fig. 9(b)) However, in the entire measurement area, MPPS is found to be 2 μm, which is quite a large diameter. The reuse filter reduces filter efficiency by up to 93.3%, which is considered a major reason for increasing total concentration of aerosol when reusing filters (Fig. 9(a)).

The HEPA filter blocks the most of aerosols, but the aerosol removal efficiency decreases gradually as filter usage time increases. The reduction of filter efficiency can increase unexpected leakage of radioactive aerosols released into the external environment and led to the internal exposure of workers. Since D&D workplace uses multiple filter systems, reducing aerosol removal efficiency of a single filter is not expected to have a significant impact on radioactive contamination in the external environment. However, workers who rely solely on a respiratory mask against radioactive aerosols can be fatal to one's health.

4.3. Relationship between filter efficiency and worker's internal exposure

According to previous researches, it is confirmed that the aerodynamic diameter distribution of aerosol depends on the chemical composition of cutting materials and has not been changed by isotopic compositions [9,35]. Therefore, the non-radiative aerosol distribution data used in the calculation of the filter efficiency is expected to be not significantly different from the radioactive aerosol distribution.

The general formulations for inhalation dose estimation are described in the following equations [36,37].

$$I = \frac{C_{air} \times BR \times T}{RP} \tag{5}$$

where I is the inhalation intake of radionuclides [Bq]; C_{air} is the airborne radionuclide concentration [Bq/m^3]; BR is the breathing rate for a worker, (i.e., an average breathing rate of 1.2 m^3/h was given in ICRP 66 publication); T is the working duration [h]; RP is the respiratory protection factor.

$$D = \sum_i (I_i \times e_i) \tag{6}$$

where D is the inhalation dose [Sv]; i is the type of radionuclide; e_i is the inhalation dose coefficient for radionuclide i [Sv/Bq].

Inhalation dose coefficient depends on the properties of aerosols such as the chemical composition of aerosols, activity median aerodynamic diameter, and the absorption rates [38,39]. For equations (5) and (6), the inhalation dose increases proportionally to radionuclide concentration and working time. By contrast, it decreases proportionally to respiratory protection efficiency.

Reduction of filter efficiency resulting from reuse or long-term use of filters can directly affect the increase in workers' internal exposure. When the test filter was reused up to 20 times, the total filter efficiency decreased by about 1%. However, even with the small reduction in filter efficiency, it is confirmed that the total aerosols mass in the downstream of filter increased significantly by about 10 times compared with using the new test filter. Therefore, if the efficiency evaluation of HEPA filter in a worker's mask is not performed properly and the worker continues to use it, there is a risk that the internal dose assessment could be underestimated by at least 10 times.

5. Conclusion

The nuclear facilities including the D&D workplace usually used several HEPA filters to prevent radioactive aerosol leakage and to keep workers safe. However, the aerosol particles cannot be completely removed by a filter because of HEPA filters have the lowest filtration efficiency in an MPPS region. In this study, it is experimentally confirmed that MPPS of filters can be formed in different areas from theoretical values, and filter efficiency continues to decrease as the number of filter usages increases. During D&D activities, the particle removal efficiency of the HEPA filter is directly related to the radiological safety of workers. For radiation safety of workers, the filter efficiency assessment will be required according to the working time.

Declaration of competing interest

The authors declare that they have no known competing financial interests or personal relationships that could have appeared to influence the work reported in this paper.

Acknowledgments

This work was financially supported by the National Research Foundation of Korea (NRF) by a grant funded by the Ministry of Science and ICT, Republic of Korea (Grant No. NRF-2017M2A8A4018596).

References

[1] S. Choi, W.I. Ko, Dynamic assessments on high level waste and low and intermediate level waste generation from open and closed nuclear fuel cycles in Republic of Korea, J. Nucl. Sci. Technol. 51 (9) (2004) 1141–1153.
[2] S. Choi, H.O. Nam, W.I. Ko, Environmental life cycle risk modeling of nuclear waste recycling systems, Energy 112 (2016) 836–851.
[3] C. Kim, S. Choi, M. Shin, Review on electro-kinetic decontamination of radioactive concrete waste from nuclear power plants, J. Electrochem. Soc. 165 (9) (2018) E330–E344.
[4] J. Severa, J. Bár, Handbook of Radioactive Contamination and Decontamination, fourth ed., vol. 47, Elsevier Science, 1991.
[5] M. Ebadian, S. Dua, H. Guha, Size Distribution and Rate of Production of Airborne Particulate Matter Generated during Metal Cutting, National Energy Technology Lab, National Energy Technology Lab., Morgantown, WV, 2001.
[6] IAEA, Radioactive Particles in the Environment: Sources, Particle Characteristics, and Analytical Techniques, IAEA-TECDOC Vienna, 2011. IAEA-TECDOC-1663.
[7] S. Choi, N. Chae, Characteristics of aerosols from different metals with plasma arc torch, in: Aerosol Technology, Bilbao, Spain, June 18-20, 2018.
[8] N. Chae, S. Choi, Review on radioactive aerosols from decommissioning on nuclear power plant, in: International Youth Nuclear Congress, Bariloche, Argentina, March 11-17, 2018.
[9] N. Chae, M.H. Lee, S. Choi, B.G. Park, J.S. Song, Aerodynamic diameter and radioactivity distributions of radioactive aerosols from activated metals cutting for nuclear power plant decommissioning, J. Hazard Mater. 369 (2019) 727–745.
[10] P. Linder, Air Filters for Use at Nuclear Facilities, Technical Reports Series No. 122, IAEA, Vienna, 1970.
[11] R.A. Sadir, C.J. Velardez, R.A. Sadir, What is HEPA? How to achieve high efficiency particulate air filtration, in: Clean Room Technology in ART Clinics, CRC Press, 2016, pp. 75–84.
[12] R.C. Brown, Air Filtration: an Integrated Approach to the Theory and Applications of Fibrous Filters, first ed., Pergamon, 1993.
[13] W.J. Kowalski, W.P. Bahnfleth, T.S. Whittam, Filtration of airborne microorganisms: modeling and prediction, ASHRAE Trans 105 (1999) 4–17.
[14] S.L. Alderman, M.S. Parsons, K.U. Hogancamp, C.A. Waggoner, Evaluation of the effect of media velocity on filter efficiency and most penetrating particle size of nuclear grade high-efficiency particulate air filters, J. Occup. Environ. Hyg. 5 (11) (2008) 713–720.
[15] T. Shimada, T. Tanaka, Characterization on the radioactive aerosols dispersed during plasma arc cutting of radioactive metal piping, J. Radioanal. Nucl. Chem. 303 (2) (2015) 1345–1349.
[16] S.H. Huang, C.W. Chen, Y.M. Kuo, C.Y. Lai, R. McKay, C.C. Chen, Factors affecting filter penetration and quality factor of particulate respirators, AAQR 13 (1) (2013) 162–171.
[17] C.C. Chen, M. Lehtimäki, K. Willeke, Aerosol penetration through filtering

facepieces and respirator cartridges, AIHA J. 53 (1992) 566–574.
[18] C.C. Chen, S.-H. Huang, The effects of particle charge on the performance of a filtering facepiece, AIHA J. 59 (1998) 227–233.
[19] S. Rengasamy, B.C. Eimer, Nanoparticle penetration through filter media and leakage through face seal interface of N95 filtering facepiece respirators, Ann. Work Exposures and Health 56 (5) (2012) 568–580.
[20] G. Smith, Nuclear Air Cleaning Handbook, U.S. DOE, Washington, DC, 2003. DOE-HDBK-1169-2003.
[21] J. Gustavsson, A. Ginestet, P. Tronville, M. Hyttinen, Air Filtration in HVAC Systems, REHVA guidebook, 2010.
[22] O. Saarela, J.E. Hulsund, A. Taipale, M. Hegle, Remaining useful life estimation for air filters at a nuclear power plant, in: 2nd Internatial Conference of the Prognostics and Health Management Society, 2014.
[23] J.H. Vincent, Aerosol Sampling: Science, Standards, Instrumentation and Applications, John Wiley & Sons, 2007.
[24] R. Baskaran, V. Subramanian, J. Misra, R. Indira, P. Chellapandi, Baldev Raj, Aerosol characterization and measurement techniques towards SFR safety studies, in: First International Conference on ANIMMA, IEEE, 2009.
[25] W.C. Hinds, Aerosol Technology: Properties, Behavior, and Measurement of Airborne Particles, John Wiley & Sons, 2012.
[26] T. Sparks, G. Chase, Filters and Filtration Handbook, sixth ed., Butterworth-Heinemann, Oxford, 2016.
[27] R. Mostofi, A. Noël, F. Haghighat, A. Bahloul, J. Lara, Y. Cloutier, Impact of two particle measurement techniques on the determination of N95 class respirator filtration performance against ultrafine particles, J. Hazard Mater. 217 (2012) 51–57.
[28] W. Bergman, J. Elliott, B. Bettencourt, J.W. Slawski, In-place HEPA Filter Penetration Test, Lawrence Livermore National Lab., 1997. UCRL-JC-127230; CONF-960715.
[29] B.G. Miller, CHAPTER 6-emissions control strategies for power plants, in: Coal Energy Systems, Academic Press, Burlington, 2005, pp. 283–392.
[30] N. Mao, Nonwoven fabric filters, in: G. Kellie (Ed.), Advances in Technical Nonwovens, Woodhead Publishing, 2016, pp. 273–310.
[31] B. Miller, Particulate formation and control technologies, in: B. Miller (Ed.), Fossil Fuel Emissions Control Technologies, Butterworth-Heinemann, 2015, pp. 145–196.
[32] K. Wark, C.F. Warner, Air Pollution: its Origin and Control. US, 1981.
[33] C.Y. Chen, Filtration of aerosols by fibrous media, Chem. Rev. 55 (3) (1955) 595–623.
[34] X. Li, H. Qin, Z. You, W. Yao, Prediction of the particles collection and pressure-drop characteristics across fibrous media, Sci. Technol. Built Environ. 24 (6) (2018) 638–647.
[35] Y. Oki, M. Numajiri, T. Suzuki, Y. Kanda, T. Miura, K. Iijima, K. Kondo, Particle size and fuming rate of radioactive aerosols generated during the heat cutting of activated metals, Appl. Radiat. Isot. 45 (1994) 553–562.
[36] R. Benke, D. Hooper, Airborne Particle Resuspension and Inhalation Radiological Dose Estimation Following Volcanic Events, CNWRA, San Antonio, Texas, 2011.
[37] E.H. Carbaugh, D.E. Bihl, J.A. Maclellan, C.L. Antonio, R.L. Hill, Methods and Models of the Hanford Internal Dosimetry Program, Pacific Northwest National Lab. (PNNL), Richland, WA, 2009. No. PNNL-15614 Rev. 1.
[38] K. Eckerman, J. Harrison, H.G. Menzel, C.H. Clement, ICRP publication 119: compendium of dose coefficients based on ICRP publication 60, Ann. ICRP 41 (2012) 1–130.
[39] IAEA, Assessment of Occupational Exposure Due to Intakes of Radionuclides, IAEA Safety Standard Series, Vienna, 1999.